Merkulova I.N., Shariya M.A., Mironov V.M., Shabanova M.S., Veselova T.N., Gaman S.A., Barysheva N.A., Shakhnovich R.M., Zhukova N.I., Sukhinina T.S., Staroverov I.I., Ternovoy S.K.
Institute of Clinical Cardiology named after A.L. Myasnikov of National Cardiology Research Center, Moscow, Russia

Computed tomography coronary angiography possibilities in "high risk" plaque identification in patients with non-ST-elevation acute coronary syndrome: comparison with intravascular ultrasound

Aim	To evaluate structural characteristics of atherosclerotic plaques (ASP) by coronary computed tomography arteriography (CCTA) and intravascular ultrasound (IVUS).
Material and methods	This study included 37 patients with acute coronary syndrome (ACS). 64-detector-row CCTA, coronarography, and grayscale IVUS were performed prior to coronary stenting. The ASP length and burden, remodeling index (RI), and known CT signs of unstable ASP (presence of dot calcification, positive remodeling of the artery in the ASP area, irregular plaque contour, presence of a peripheral high-density ring and a low-density patch in the ASP). The ASP type and signs of rupture or thrombosis were determined by IVUS.
Results	The IVUS study revealed 45 unstable ASP (UASP), including 25 UASP with rupture and 20 thin-cap fibroatheromas (TCFA), and 13 stable ASP (SASP). No significant differences were found between distribution of TCFA and ASP with rupture among symptom-associated plaques (SAP, n=28) and non-symptom-associated plaques (NSAP, n=30). They were found in 82.1 and 73.3% of cases, respectively ($p>0.05$), which indicated generalization of the ASP destabilization process in the coronary circulation. However, the incidence of mural thrombus was higher for SAP (53.5 and 16.6% of ASP, respectively; $p<0.001$). There was no difference between UASP and SASP in the incidence of qualitative ASP characteristics or in values of quantitative ASP characteristics, including known signs of instability, except for the irregular contour, which was observed in 92.9% of UASP and 46.1% of SASP ($p=0.0007$), and patches with X-ray density ≤46 HU, which were detected in 83.3% of UASP and 46.1% of SASP ($p=0.01$). The presence of these CT criteria 11- and 7-fold increased the likelihood of unstable ASP (odd ratio (OR), 11.1 at 95% confidence interval (CI), from 2.24 to 55.33 and OR, 7.0 at 95% CI, from 5.63 to 8.37 for the former and the latter criterion, respectively).
Conclusion	According to IVUS data, two X-ray signs are most characteristic for UASP, the irregular contour and a patch with X-ray density ≤46 HU. The presence of these signs 11- and 7-fold, respectively, increases the likelihood of unstable ASP.

Keywords	Acute coronary syndrome; coronary computed tomography angiography; intravascular ultrasound; coronary artery; unstable atherosclerotic plaque; remodeling index; minimum density of atherosclerotic plaques
For citation	Merkulova I.N., Shariya M.A., Mironov V.M., Shabanova M.S., Veselova T.N., Gaman S.A. et al. Computed tomography coronary angiography possibilities in "high risk" plaque identification in patients with non-ST-elevation acute coronary syndrome: comparison with intravascular ultrasound. Kardiologiia. 2020;60(12):64–75. [Russian: Меркулова И.Н., Шария М.А., Миронов В.М., Шабанова М.С., Веселова Т.Н., Гаман С.А. и др. Возможности компьютерной томографии в выявлении атеросклеротических бляшек высокого риска у больных с острым коронарным синдромом без подъема сегмента ST: сопоставление с внутрисосудистым ультразвуковым исследованием. Кардиология. 2020;60(12):64–75]

Corresponding author Merkulova I.N. E-mail: irina_merkulova@list.ru

Gradually progressing stenosing coronary atherosclerosis is a major factor in angina attacks in patients with chronic coronary heart disease (CHD). A different mechanism of coronary attacks is observed in patients with acute coronary syndrome (ACS), usually acute mural coronary thrombosis resulting from the rupture or erosion of the so-called vulnerable or unstable atherosclerotic plaque (ASP) or high-risk ASP, leading to sudden coronary obstruction or even occlusion [1–4]. For this reason, when examining ACS much attention is paid to structural features and properties of ASPs responsible for the coronary attack and potentially unstable plaques throughout the coronary bed. Of all the histological types of ASP,

ISSN 0022-9040. Kardiologiia. 2020;60(12). DOI: 10.18087/cardio.2020.12.n1304

thin-cap fibroatheroma (TCFA) is the most prone to rupture. It has a large lipid-necrotic nucleus and thin (65 microns) cap [5].

There are currently various invasive and non-invasive coronary artery imaging methods used to investigate coronary ASPs [6]. Coronary computed tomography angiography (CCTA) is the most widely used non-invasive method due to its relative safety, the possibility of a cross-sectional examination of the entire coronary bed, good reproducibility, and relatively high accuracy of assessing stenosis and ASP dimensions [7–11].

However, special attention is also paid to the possibilities of CCTA in detecting high-risk ASPs. CCTA resolution does not show the thin cap of a TCFA, but optical coherence tomography (OCT) does. Intravascular ultrasound examination (IVUS) with spectral analysis confirms the presence of a thin cap indirectly. Since the method of investigating an ASP structure in CCTA is based on the differentiation of vascular wall tissues with different radiographic densities from the density of a contrast agent in the vascular lumen, one of the areas of examining vulnerable plaques is to quantify the density of the structural components of different types of plaques, including TCFA, found mostly by IVUS [12–16]. Plaques with a large lipid nucleus were expected to differ significantly from calcified and fibrous plaques in density.

Several trials also showed that some CT signs of ASPs are associated with a high risk of developing ACS. These signs include positive remodeling, low radiographic density of a plaque (<30 HU), a ring of high attenuation around the plaque, and the presence of microcalcification (less than 3 mm) in the soft tissue of the plaque [17–24]. Contour irregularity, another sign of unstable ASPs, is described in the Russian literature [25]. Therefore, one of the research areas of vulnerable ASP was to evaluate the above-mentioned CT signs or their combinations as surrogate markers of such plaques verified by IVUS or OCT [13, 26–33]. However, the results of these studies are controversial, including the definition, and which CT signs of instability and their combinations are the most accurate markers of vulnerable plaques and whether they are or not.

Objective

To assess structural characteristics of ASPs using CCTA and IVUS and the capabilities of CCTA to identify high-risk ASPs verified by IVUS.

Material and methods

Over a period of two years of prospective recruitment and after exclusion for the reasons described below, 37 patients diagnosed with ACS at hospitalization were included in the study. Inclusion criteria were: an angina attack lasting more than 20 minutes or clinical manifestations of unstable angina (UA), newly onset, progressing, or early post-infarct angina. Patients who had undergone coronary artery or mammaro-coronary bypass grafting, with severe renal impairment (glomerular filtration rate <45 mL/min/1.73 m^2), history of allergic reactions to radiographic medication, persistent atrial fibrillation, severe complications of the underlying disease (cardiogenic shock, acute heart failure Killip III–IV functional class), and severe concomitant diseases were excluded from the study. Patients with intact coronary arteries or stenosis less than 25%, massive calcification (coronary artery calcium ≥600 HU) on CCTA, low image quality, non-coronary cause of chest pain were also excluded. Thus, 37 patients aged 34–72 years were included in the final analysis of the ASP condition. Non-ST-segment elevation myocardial infarction (MI) was diagnosed in 13 patients, and UA was diagnosed in 24 patients. The clinical characteristics of patients who underwent CCTA, coronary angiogram (CAG), and IVUS are shown in Table 1.

Clinical examination included laboratory tests (including cardiac-specific troponin and creatine kinase-MB), electrocardiogram (ECG), Holter monitoring, echocardiography.

CT was performed on a 64-slice CT scanner Aquillion 64 with intravenous administration of non-ionic iodinated contrast agent following the standard protocol. Topogram was performed to assess the area of interest, native and arterial phases. The types and parameters of ASPs were assessed: length, outline, burden (plaque area as a percentage of the narrowest cross-section area of the artery), remodeling index (RI) calculated as:

$$RI=D1/D2,$$

where D1 is the outer diameter of the coronary artery at the plaque level, D2 is the outer diameter of the reference segment (the nearest proximal, if absent, distal intact segment).

Positive remodeling at the plaque level was regarded as RI ≥1,05. All the previously described CT signs of plaque instability were assessed. The analysis excluded coronary segments with low image quality and outer diameter less than 1.5–2 mm.

For all patients undergoing diagnostic CAG (radial approach, Allura Xper FD 10), IVUS of coronary arteries was also performed by means of an iLab IVUS Console scanner using an Atlantis 40 MHz

intravascular ultrasound transducer and iMap spectral analysis following the standard protocols. The sensor's length covered the area of interest in the proximal and middle coronary sections with a length of 110 mm. IVUS was not performed in arteries with more than 90% stenosis due to the risk of complications. The types of ASPs were defined visually during IVUS in grayscale and automatically using software – a spectral analysis function (automatic color-coding of plaque components) [34]. Patients signed informed consent before performing studies.

The comprehensive clinical investigation identified symptom-related plaques (SRPs) and symptom-free plaques (SFPs) visible on IVUS. In the CCTA, CAG, and IVUS analysis. Only one plaque was considered as SRP in all cases, which was detected in the artery supplying the site of myocardial infarction or ischemia, established by means of ECG, echocardiography (local contractility impairment), and invasive CAG. If several ASPs are detected in the artery, the plaque responsible for the most significant stenosis of the vascular lumen [35], especially if there are signs of mural thrombosis, was considered SRP.

Statistical analysis was performed using Microsoft Excel 2013 and MedCalc v. 2.7. Medians and interquartile ranges were calculated for quantitative parameters. Analysis of correlation dependence of the ASP characteristics of interest was performed using Spearman's rank correlation coefficient. The differences were statistically significant at $p<0.05$. The frequency tables and 2×2 contingency tables using Fisher's exact test (bilateral distribution) to assess the significance were used to compare qualitative parameters. The binary classification of ASPs (stable – 0 and unstable – 1) was based on the ROC-analysis of the X-ray density of ASPs determined during the CT and the calculation of the so-called optimal (threshold) value distinguishing stable and unstable ASPs. The gold standard for ROC-analysis was the IVUS-based classification of ASPs. Multi-factor analysis of the assessment of ASP instability signs was performed using logistic regression. Odds ratio (OR) was additionally determined, i.e., the relative risk of ASP instability in the presence/absence of CT signs of instability.

Results

Characteristic of atherosclerotic plaques in patients with ACS according to CCTA

Analysis of structural characteristics of 60 visible ASPs according to CCTA and IVUS was carried out in 37 patients. The plaque assessment with CCTA was performed before the processing of IVUS results.

Table 1. General characteristic of patients who underwent CTA, CAG, and IVUS (n = 37)

Parameter		Value
Male		29 (78.4)
Mean age, years		58 [44; 65]
Alimentary obesity		9 (24.3)
Body mass index, kg/m2		27 [24; 29]
Smoking		20 (54)
Burdened family history		11 (29.7)
Arterial hypertension		23 (62.2)
Diabetes mellitus		2 (5.4)
History of MI		10 (27)
Elevated total cholesterol		15 (40.5)
Mean cholesterol level, mmol/L		4.89 [4.17; 5.39]
Elevated triglyceride levels		8 (21.6)
Mean triglyceride levels, mmol/L		1.58 [0.94; 2.20]
Coronary artery disease course	Acute MI	13 (35.2)
	UA	24 (64.8)

The data is presented as an absolute number (%) or the median [interquartile range]. CAG, coronary angiography; IVUS, intravascular ultrasound study; MI, myocardial infarction; UA, unstable angina.

According to the standard classification of ASP types by CCTA, 32 (53%) soft, 25 (42%) combined, and 3 (5%) calcified ASPs were detected in 60 affected areas. All calcified ASPs were excluded from subsequent analysis of the CCTA results, since standard signs of instability could not be identified. The structural characteristics and signs of instability in soft and combined ASPs are given in Figure 1. All ASPs were divided into two groups: SRPs (n=28) and SFPs (n=29). The comparison of SRPs and SFPs based on CT data is shown in Table 2.

Characteristics of atherosclerotic plaques in patients with ACS according to IVUS

The standard analysis of the same 60 affected coronary segments using grayscale IVUS detected 25 ruptured ASPs, 33 ASPs without rupture, 1 spontaneous dissection, and 1 intramural hematoma. The last two types of lesions were later excluded from the analysis.

Mural thrombosis was observed on the surface of 20 (34.5%) of 58 ASPs.

IVUS with spectral analysis identified four types of ASPs in accordance with the standard classification [34]. Examples are shown in Figure 2. TCFA contains a large lipid necrotic nucleus, and fibrous tissue is not detected in some areas between the ASP lumen and the lipid necrotic component, which is a sign of a damaged cap.

A cComparison of grayscale IVUS data with the spectral analysis function allowed 22 ruptured ASPs

ISSN 0022-9040. Kardiologiia. 2020;60(12). DOI: 10.18087/cardio.2020.12.n1304

Figure 1. CCTA. Multiplanar reconstructions (A, B, C) and transverse slices of coronary arteries at the ASP level (D, E, F, G): X-ray characteristics of ASPs

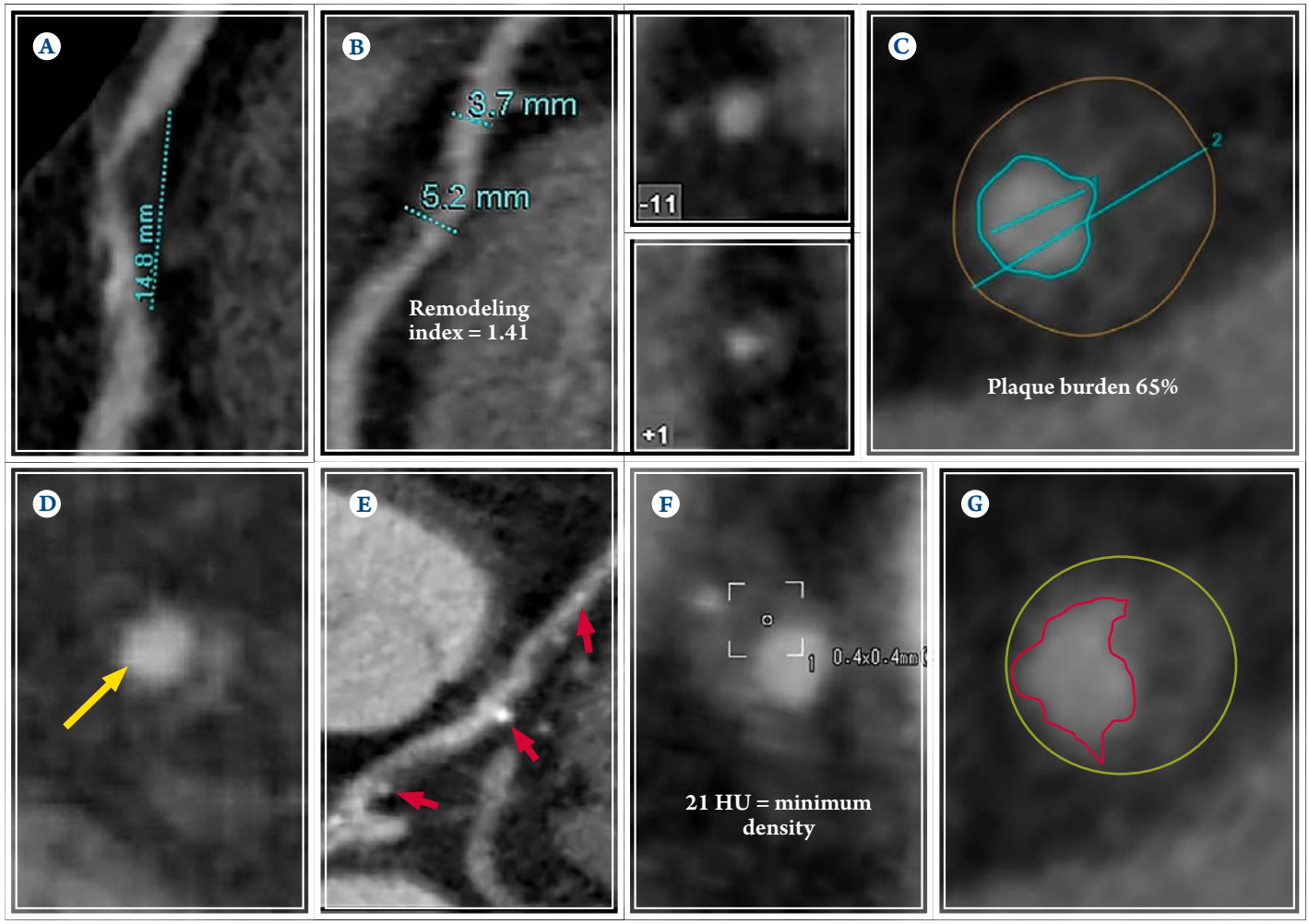

A – length of an ASP; B – left: positive remodeling of the artery at ASP level; right: transverse sections of the artery at the reference level (top) and maximum lumen narrowing (bottom); **C** – the burden of the plaque; **D** – a ring of attenuation around the ASP (yellow arrow); **E** – pinpoint calcification – less than 0.3 cm (red arrows); **F** – hypodense site (minimum X-ray density in the area of interest); **G** – the irregular contour of the ASP. CCTA, Coronary computed tomography angiography; ASP, atherosclerotic plaque.

detected by the greyscale IVUS to be determined as incorrectly classified as TCFA by IVUS with spectral analysis, since plaque rupture is not visible by means of color-coding. Figure 3 shows an example of the complex analysis of such plaque with both signs of rupture (A) and structural components typical of TCFA, particularly a large lipid necrotic nucleus (yellow-pink component), which occupies more than 50% of the

Table 2. CCTA characteristics of soft and combined SRPs and SFPs

Parameter	SRPs (n = 28)	SFPs (n = 29)	p
Length, mm	19 [15; 30]	16 [11; 24]	0.144
Burden, %	78.7 [58.7; 86.2]	66.2 [55.0; 71.7]	0.029
Positive artery remodeling	14 (50)	12 (41.4)	0.599
Remodeling index	1.14 [1.00; 1.25]	1.10 [1.00; 1.14]	0.167
Contour irregularity	27 (96)	20 (72)	0.025
Pinpoint calcification	11 (39)	11 (38)	1.000
Ring attenuation	16 (28)	6 (10)	0.007
Low X-ray density site in all plaques, HU	31 [12; 45]	31 [22; 53]	0.482

The data is presented as an absolute number (%) or the median [interquartile range].
CCTA, Coronary computed tomography angiography; SRP, symptom-related plaque; SFP, symptom-related plaques.

Figure 2. Types of ASPs (color-coded IVUS: transverse slices at the ASP level)

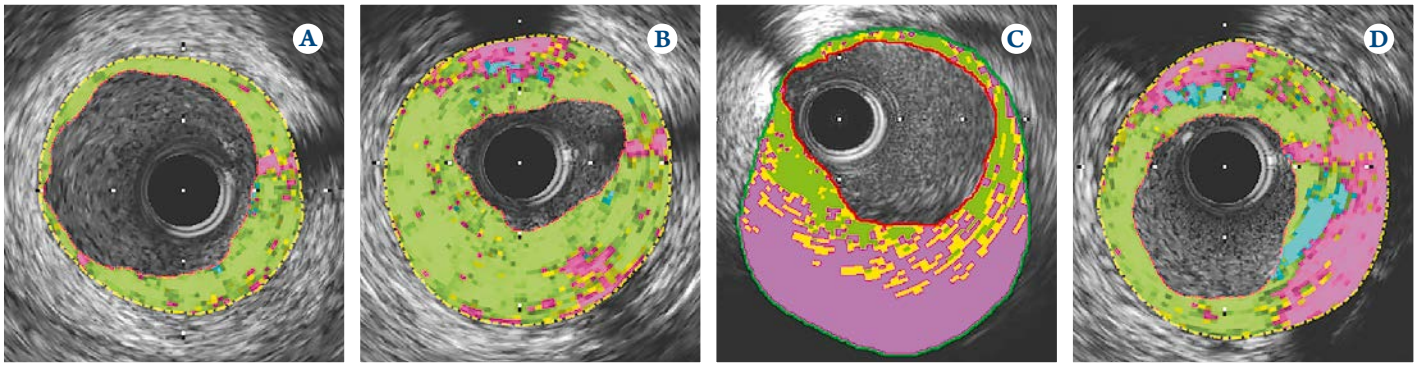

A – fibrous plaque; **B** – thick-cap fibroatheroma; **C** – thin-capsule fibroatheroma; **D** – calcified fibroatheroma.
ASP, atherosclerotic plaque; IVUS, intravascular ultrasound study.

plaque (B). CAG showed no signs of rupture in the same ASP (B).

Thus, IVUS detected 22 ruptured TCFAs, 20 TCFAs, 12 thick-cap fibroatheromas (including 2 ruptured ones), 2 fibrous plaques, and 2 calcified fibroatheromas (including 1 ruptured one). No ASPs of any other type, pathological intima thickening, were detected. The mural thrombotic masses were determined in 14 ruptured TCFA, 5 TCFAs without rupture, 1 ruptured thick-capsule fibroatheroma.

We also classified all detected ASPs by IVUS to SRPs (n=28) and SFPs (n=30). The ruptured ASP were more frequent among SRPs compared to SFPs: n=15 (53.5%) and n=10 (33.3%), and TCFA and thick-cap fibroatheromas were more frequent among SFPs: n=12 (40.0%) and n=8 (26.6%) compared to SRPs: n=8 (28.5%) and n=2 (7.0%). However, there are no significant differences in the rate of these ASP types among SRPs and SFPs (p>0.05). It should be noted that thrombosis was statistically more frequent in SRPs compared to SFPs: n=15 (53.5%) and n=5 (16.6%; p=0.005).

Estimation of the minimum X-ray density as a CT marker of APS instability

During IVUS, 20 TCAFs and 25 ruptured ASPs were classified as unstable ASPs, 88% of which were also TCAFs before the rupture. The remaining 13 ASPs were considered stable. Among the unstable and stable ASPs, the number of soft [25 (55.5%) and 5 (38.5%); p=0.352] and combined [17 (37.7%) and 8 (61.5%); p=0.203] plaques did not differ to a statistically significant degree.

One of the main signs of TCFA as high-risk ASPs is the presence of a large lipid nucleus, evidenced by sites with low minimum X-ray density in plaques on CT, since the nucleus density is much lower than the density of other components. The minimum X-ray

Figure 3. Results of the complex analysis of a ruptured plaque

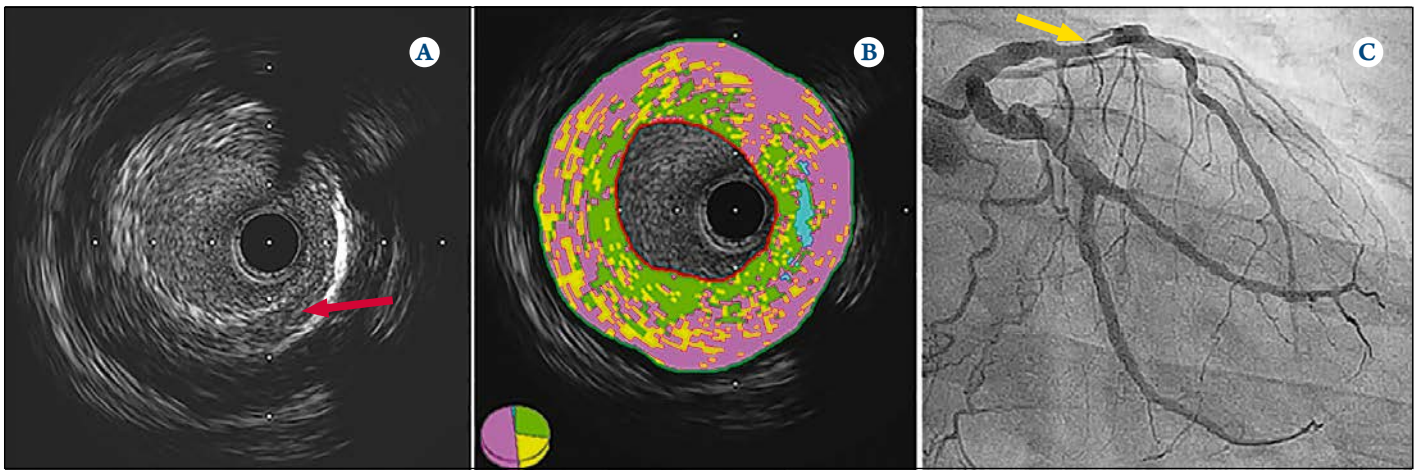

A – gray scale IVUS: Rupture ASP (red arrow); **B** – IVUS with spectral analysis: TCFA; **C** – CAG: moderate stenosis in the middle LAD segment (yellow arrow).
ASP, atherosclerotic plaque; IVUS, intravascular ultrasound study; TCFA, thin-capsule fibroatheroma;
CAG, coronary angiography; LAD, left anterior descending artery.

ISSN 0022-9040. Kardiologiia. 2020;60(12). DOI: 10.18087/cardio.2020.12.n1304

Table 3. CT characteristics of unstable and stable ASPs

Parameter	Unstable ASPs according to IVUS (n = 42)	Stable ASPs according to IVUS (n = 13)	p
Contour irregularity	39 (92.9)	6 (46.1)	0.0007
Minimum density ≤46 HU	35 (83.3)	6 (46.1)	0.01
Burden, %	70 [60.6; 84.4]	65 [51.9; 70.0]	0.071
Microcalcification	16 (38.1)	3 (23.1)	0.506
Positive remodeling	20 (47.6)	4 (30.8)	0349
Remodeling index	1.1 [1.01; 1.23]	1.01 [1.00; 1.14]	0.119
Ring attenuation	19 (45.2)	3 (23.1)	0.203

The data is presented as an absolute number (%) or the median [interquartile range].
ASP, atherosclerotic plaque; IVUS, intravascular ultrasound study.

density of plaques, which were unstable according to IVUS (28 [12; 41] HU, n = 42) was expectedly to be lower than in stable ones to a statistically significant degree (47 [25.8; 62.5] HU, n = 13; p = 0.04), calcified plaques were not taken into account. The X-ray density of ≤46 HU turned out to be optimal (threshold) for differentiation of unstable ASPs ((Figure 4, A; Table 3). Sensitivity, specificity, positive predictive value (PPV), and negative predictive value (NPV) for unstable ASPs according to IVUS were 81.4%, 58.8%, 83.3%, and 55.6%, respectively (Figure 4, B). Moreover, the presence of a site with an X-ray density of ≤ 46 HU in the ASP increases the probability of its instability (OR 7.0, 95% confidence interval (CI) 5.63–8.37) 7-fold.

Detection of CT signs of instability in unstable plaques by IVUS

In CCTA, irregular contours and the sites with a minimum X-ray density of ≤46 HU were statistically more frequent in the group of unstable plaques. According to the rest of the CT signs of instability there are no valid intergroup differences (see Table 3). However, a high attenuation ring around the plaque was more frequent in ruptured TCFAs than in TCFAs, 63.6 and 25% of cases, respectively (p = 0.015).

The detection of contour irregularity confirmed the presence of unstable plaque with sensitivity, specificity, PPV, and NPV equal to 92.8%, 46.1%, 84.8%, and 66.7%, respectively (Figure 5). This sign increases the

Figure 4. Minimum X-ray density in unstable and stable ASPs

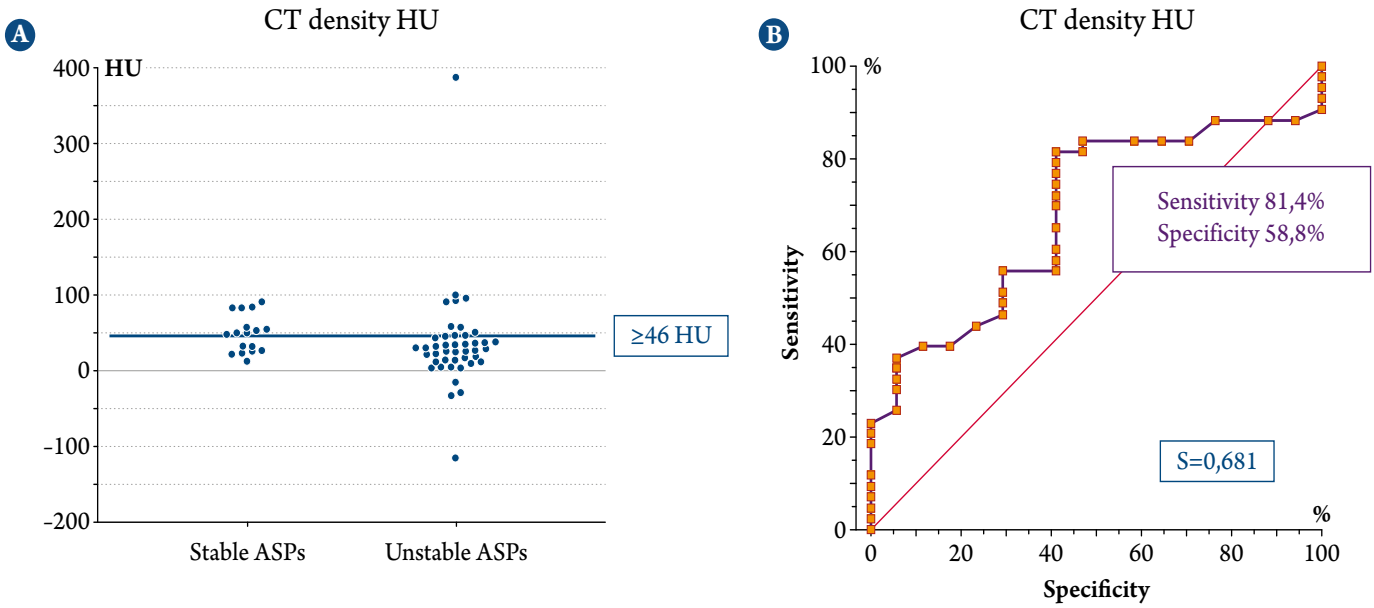

A – distribution of the minimum X-ray density in unstable and stable ASPs (X-ray density threshold is 46 HU); HU, Hounsfield units.
B – ROC curve used to calculate minimum X-ray density threshold according to CCTA for the prognosis of an unstable plaque by IVUS.
ASP, atherosclerotic plaque; CCTA, coronary computed tomography angiography; IVUS, intravascular ultrasound study.

possibility of plaque instability up to 11 times (OR 11.1, 95% CI 2.24–55.33; p<0.009).

Discussion

The study assessed the role of CCTA in identifying ASP components and signs of instability in a total of 60 plaques in 50 coronary arteries of 37 patients with ACS. One of its advantages is the comprehensive use of IVUS, both grayscale (to identify ruptures, thrombosis), and with spectral analysis (to define ASP types) as a method with a greater resolution than that of CCTA. This not only identifies ASP components in detail (including high-risk ASP), but also verifies CCTA accuracy of assessing structural features in ACS. The analysis of CCTA capabilities in detecting unstable ASPs verified by IVUS and evaluating the known CCTA instability signs as markers of high-risk ASPs are described for the first time in the Russian literature. The analysis of CCTA data intentionally included only non-calcified or partially calcified plaques, since the soft-tissue component is known to be primarily an alteration substrate. These CT types of plaques are more common in ACS on the one hand, while, on the other, assessing CT signs of instability in calcified plaques is either impossible or challenging due to massive calcification artifacts. The study is limited by the fact that the analysis did not include ASPs, especially SRP, which were inaccessible to the ultrasound transducer. This was due to the minimum lumen area, and plaques that narrow the lumen by less than 25%, usually immature, intima thickening and fibroatheromas in patients with ACS [36, 37].

The absence of significant intergroup differences in some ASP characteristics on CCTA in patients with ACS when comparing SRPs and SFPs (positive arterial remodeling at the plaque level, spot calcification, sites with minimal X-ray density, etc.) can be caused by the generalization of plaques destabilization throughout the coronary bed, rather than only the symptom-related artery. This has been described by several authors who applied various methods of ASP visualization and showed that vulnerable plaques are found both among SRPs and SFPs [36, 38–41]. The above-mentioned signs reflect the plaque's potential for sudden changes rather than the fact of changes. The more significant burden in SRPs, more frequent detection of such CT signs as contour irregularity, a ring of high attenuation around the plaque, are, on the contrary, naturally correlated with the processes directly leading to ACS, such as plaque rupture, thrombosis, subsequently increased burden of the plaque and progressing coronary obstruction. Data from the literature and IVUS in our study also showed the correlation of these signs to plaque rupture and thrombosis. Mural thrombosis and a ring of high attenuation around plaque were statistically significantly more frequent in SRPs and ruptured ASPs, respectively [13, 42].

The classification of ASP types by IVUS and OCT corresponds to the histological classification [43], according to which two types of mature ASPs, TCFA and ruptured ASP, are classified as unstable ASPs [44, 45]. The comprehensive analysis of the IVUS data identified different ASP types and distinguished TCFAs as ASPs (also mainly TCFAs) prone to rupture but with intact fibrous caps from ruptured ASP.

According to our study, the ruptured ASPs and TCFAs prevailed among mature non-calcified coronary plaques in patients with ACS, which corresponds to the literature [46, 47].

There are no significant differences in the prevalence of TCFAs, thick-cap fibro-atheromas, and ruptured ASPs between SRPs and SFPs. This corresponds to the mentioned hypothesis of ASP destabilization generalization throughout the coronary bed. According to IVUS, the only difference between SRPs and SFPs was the more frequent detection of mural thrombi in SRPs. IVUS is considered not to visualize small thrombi, which is a limitation of the method. However, IVUS is used in several studies, including ours, to detect thrombi on the surface of coronary ASPs [48, 49].

Figure 5. Sensitivity and specificity of the CT sign contour irregularity used to determine ASP instability by IVUS

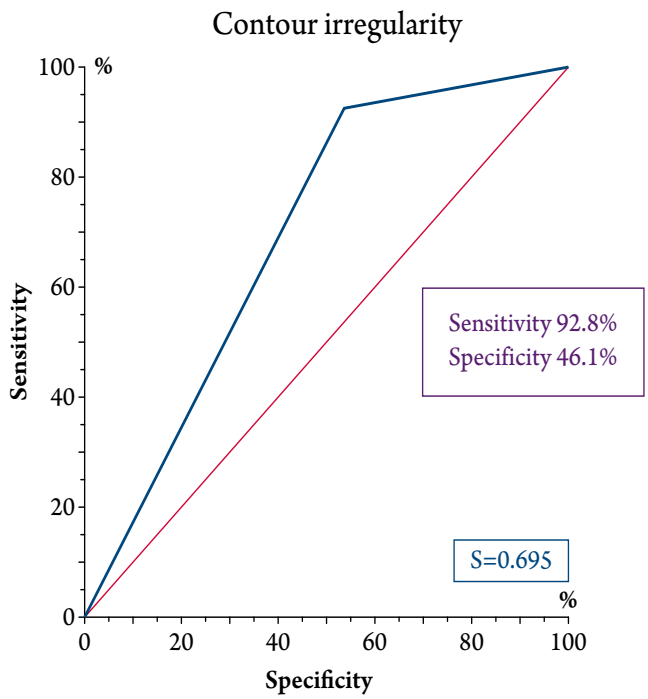

CT, computed tomography; ASP, atherosclerotic plaque; IVUS, intravascular ultrasound study.

ISSN 0022-9040. Kardiologiia. 2020;60(12). DOI: 10.18087/cardio.2020.12.n1304

Эдарби® Кло

азилсартана медоксомил + хлорталидон

МОЩНЫЙ СОЮЗ

ДЛЯ СНИЖЕНИЯ АД
В ТЕЧЕНИЕ 24 ЧАСОВ[1, 2]

АЗИЛСАРТАН

ПРЕВОСХОДИТ ДРУГИЕ САРТАНЫ*
В АНТИГИПЕРТЕНЗИВНОМ ЭФФЕКТЕ[3, 4]

ХЛОРТАЛИДОН

ИМЕЕТ ОБШИРНУЮ ДОКАЗАТЕЛЬНУЮ БАЗУ[5–9]
ПО СНИЖЕНИЮ РИСКА ССО**
У ПАЦИЕНТОВ С АГ

STADA

Наша миссия – ваше здоровье

МОЩНЫЙ СОЮЗ

НОВИНКА

*По сравнению с валсартаном и олмесартаном. ** ССО – сердечно-сосудистые осложнения. **1.** Инструкция по применению лекарственного препарата для медицинского применения Эдарби® Кло, таблетки, покрытые плёночной оболочкой, 40 г + 12,5 мг, 40 мг + 25 мг. Рег. уд. ЛП-002941 от 02.04.2015. **2.** Cushman W.C., et al. Hypertension. 2012; 60: 310–318. **3.** Sica D., et al. J. Clin. Hypertens. 2011; 13: 467–472. **4.** White W.B., et al. Hypertension. 2011; 57: 413–420. **5.** Hypertension Detection and Follow-up Program Cooperative Group. JAMA. 1979; 242: 2562–2571. **6.** Multiple Risk Factor Intervention Trial Research Group. Circulation. 1990; 82: 1616–1628. **7.** Dorsch M.P., et al. Hypertension. 2011; 51: 689–694. **8.** SHEP Cooperative Research Group. JAMA. 1991; 265: 3255–3264. **9.** ALLHAT Officers and Coordinators for the ALLHAT Collaborative Research Group. JAMA. 2002; 288: 2981–2997.

Сокращённая информация по применению
Торговое название: Эдарби® Кло. **Международное непатентованное или группировочное название:** азилсартана медоксомил + хлорталидон. **Лекарственная форма и дозировка:** таблетки, покрытые плёночной оболочкой, 40 мг + 12,5 мг; 40 мг + 25 мг. **Показания к применению:** эссенциальная гипертензия (пациентам, которым показана комбинированная терапия). **Противопоказания:** повышенная чувствительность к действующим веществам и другим компонентам препарата; рефрактерная гипокалиемия; рефрактерная гипонатриемия; анурия; беременность и период грудного вскармливания; одновременный приём препаратов, содержащих алискирен, у пациентов с сахарным диабетом и/или умеренными и тяжёлыми нарушениями функции почек (скорость клубочковой фильтрации (СКФ) менее 60 мл/мин/1,73 м^2 площади поверхности тела); одновременное применение с ингибиторами АПФ у пациентов с диабетической нефропатией; тяжёлые формы сахарного диабета; возраст до 18 лет (эффективность и безопасность не установлены); нарушения функции печени тяжёлой степени (более 9 баллов по шкале Чайлд-Пью) (отсутствует опыт применения); почечная недостаточность тяжёлой степени (клиренс креатинина (КК) менее 30 мл/мин) (отсутствует опыт применения). **Способ применения и дозы.** Препарат Эдарби® Кло принимают внутрь один раз в сутки независимо от времени приёма пищи. Рекомендованная начальная доза препарата Эдарби® Кло составляет 40 мг азилсартана медоксомила + 12,5 мг хлорталидона 1 раз в сутки. При необходимости дополнительного снижения АД дозу препарата Эдарби® Кло можно увеличить до максимальной: 40 мг азилсартана медоксомила + 25 мг хлорталидона 1 раз в сутки. Препарат Эдарби® Кло следует принимать ежедневно, без перерыва. В случае прекращения лечения пациент должен сообщить об этом врачу. **Побочное действие:** для комбинации азилсартана медоксомила и хлорталидона: очень часто: повышение концентрации креатинина; часто: головокружение, постуральное головокружение, обморок (синкопе), выраженное снижение АД, диарея, тошнота, гиперурикемия, повышение концентрации мочевины, повышенная утомляемость, периферические отёки; для хлорталидона (монотерапия): очень часто: гиперлипидемия, гипокалиемия; часто: выраженное снижение АД, потеря аппетита, желудочно-кишечные расстройства, крапивница, снижение потенции, гипомагниемия; для азилсартана медоксомила (монотерапия): часто: головокружение, диарея, повышение активности креатинфосфокиназы. **Полный перечень побочных эффектов содержится в инструкции по применению. С осторожностью:** тяжёлая хроническая сердечная недостаточность (IV функциональный класс по классификации NYHA); нарушение функции почек (КК более 30 мл/мин); нарушение функции печени лёгкой и умеренной степени (5–9 баллов по шкале Чайлд-Пью); двусторонний стеноз почечных артерий и стеноз артерии единственной функционирующей почки; ишемическая кардиомиопатия; ишемические цереброваскулярные заболевания; состояние после трансплантации почки; состояния, сопровождающиеся снижением объёма циркулирующей крови (в том числе рвота, диарея, приём высоких доз диуретиков), а также у пациентов, соблюдающих диету с ограничением поваренной соли; первичный гиперальдостеронизм; гиперурикемия и подагра; бронхиальная астма; системная красная волчанка; стеноз аортального и митрального клапана; гипертрофическая обструктивная кардио-миопатия; возраст старше 75 лет; гипокалиемия, гипонатриемия. **Полная информация по препарату содержится в инструкции по медицинскому применению.**

АО «Нижфарм», Россия, 603950,
г. Нижний Новгород, ул. Салганская, 7.
Тел.: +7 (831) 278 80 88,
E-mail: med@stada.ru.
www.stada.ru

Дата выхода материала ноябрь 2020 г.
6666822002MO0073

Since one of the main signs of TCFA is the presence of a large lipid nucleus with the lowest X-ray density compared to other plaque components, many studies in the search for surrogate CT markers of this type of ASP were focused on identifying the range of the minimum plaque X-ray density. Later studies investigated the amount of the non-calcified component as possible radiographic signs of vulnerable plaques [12–16, 33]. According to our study, the X-ray density of unstable plaques in IVUS was also significantly lower than the density of the rest ASPs, while the level of 46 HU was an optimal threshold of differentiating stable and unstable plaques. Our findings are almost the same as the findings of another study, which used an advanced technique of identifying high-risk plaques [49]. The X-ray density thresholds for unstable plaques differ from study to study, and there is no standard value for individual density differentiation. Moreover, the ranges of individual values overlap in the unconditional significance of intergroup differences in the X-ray density values of different plaque components, such as lipid necrotic and fibrous, making it difficult to estimate what type a non-calcified plaque belongs. However, further improvements, including the determination of the low-density component volumes, have been made in this area, such as hardware and software improvements [13, 49–53], and new CT signs of high-risk plaques are being investigated [53–56].

Several studies have shown the correlation with ACS of such CT-signs as positive remodeling, the presence of sites < 30 HU, microcalcification, a ring of high attenuation around the plaque, and irregular contours, although the data is contradictory [13, 26–33]. These signs are also referred to as CT signs of ASP instability but are not synonymous with signs of unstable plaques according to the histological classification. We estimated their detection rate in unstable and stable plaques according to IVUS, except for the minimum density <30 HU, as we used a threshold density of ≤46 HU instead. There were statistically significant differences between the groups only in the rate of this criterion (p=0.01) and contour irregularity (p=0.0007). According to our findings, the minimum X-ray density of ≤46 HU is characterized by average sensitivity and specificity, but is 7-times higher than the probability of plaque being unstable. Contour irregularity is characterized by high sensitivity but low specificity in detecting unstable ASPs. However, this sign is 11-times higher than the probability of the plaque being unstable. Contour irregularity as a clinically significant criterion of coronary ASP instability in ACS has been previously discussed in the Russian literature [25], but its was verified by IVUS for the first time in this study.

The values of the remaining radiographic signs in unstable ASPs were higher than in stable ones, but the differences did not reach statistical significance, corresponding to some other studies [13, 32, 33, 57, 58]. It should be noted that a ring of high attenuation was detected around the ruptured ASPs significantly more often than in TCFAs, corresponding to the data of other authors [13, 58].

Conclusion

CCTA is an informative non-invasive method of assessing the ASP components, including detecting plaques with signs of instability. This was confirmed in our study by a comparative analysis of the reference IVUS findings.

The comprehensive analysis of intravascular ultrasound in grayscale and with spectral analysis was preferable to the use of spectral analysis only, since it allowed us to identify ASP types, ruptures, and mural thrombosis in plaques.

The absence of difference between SRPs and SFPs in the rate of detecting different types of ASBs in patients with ACS, including TCFAs and ruptured ASPs, as well as such CT characteristics of ASPs as positive arterial remodeling at the plaque level, spot calcification, low X-ray density sites, and others, corresponds to the hypothesis of the ASP destabilization generalization throughout the coronary bed, and not only in SRPs. Significantly higher values of SRP burden, more frequent detection of such CT signs as contour irre-gularity, a ring of high attenuation around the plaque, are, on the contrary, naturally associated with the processes directly leading to ACS: plaque rupture, thrombosis, subsequent deterioration of coronary obstruction. This is confirmed by the more frequent detection of mural thrombi in SRPs, when compared to SFPs (58% and 15.6%, respectively, p = 0.0005), and a ring of high attenuation around ruptured plaques.

According to our study, contour irregularity and a low X-ray density site of ≤46 HU are the most typical CT signs of unstable plaques. The two signs increase the probability of the plaque being unstable 11- and 7-fold, respectively.

Further improvement of hardware, software, evaluation of the significance of new CT criteria of plaque vulnerability gives hope for the further improvement of CCTA accuracy in assessing ASPs.

No conflict of interest is reported.

The article was received on 01/08/2020

ISSN 0022-9040. Kardiologiia. 2020;60(12). DOI: 10.18087/cardio.2020.12.n1304

REFERENCES

1. Falk E. Morphologic features of unstable atherothrombotic plaques underlying acute coronary syndromes. The American Journal of Cardiology. 1989;63(10):E114–20. DOI: 10.1016/0002-9149(89)90242-7
2. Virmani R, Burke AP, Farb A, Kolodgie FD. Pathology of the Vulnerable Plaque. Journal of the American College of Cardiology. 2006;47(8):C13–8. DOI: 10.1016/j.jacc.2005.10.065
3. Fuster V, Badimon JJ, Chesebro JH. Atherothrombosis: mechanisms and clinical therapeutic approaches. Vascular Medicine. 1998;3(3):231–9. DOI: 10.1177/1358836X9800300310
4. Farb A, Tang AL, Burke AP, Sessums L, Liang Y, Virmani R. Sudden Coronary Death: Frequency of Active Coronary Lesions, Inactive Coronary Lesions, and Myocardial Infarction. Circulation. 1995;92(7):1701–9. DOI: 10.1161/01.CIR.92.7.1701
5. Kolodgie FD, Burke AP, Farb A, Gold HK, Yuan J, Narula J et al. The thin-cap fibroatheroma: a type of vulnerable plaque: The major precursor lesion to acute coronary syndromes: Current Opinion in Cardiology. 2001;16(5):285–92. DOI: 10.1097/00001573-200109000-00006
6. Celeng C, Takx RAP, Ferencik M, Maurovich-Horvat P. Non-invasive and invasive imaging of vulnerable coronary plaque. Trends in Cardiovascular Medicine. 2016;26(6):538–47. DOI: 10.1016/j.tcm.2016.03.005
7. Shabanova M.S. Comparison of coronary stenosis degree measurements with computed tomography, intravascular ultrasound and coronary angiography. Russian Electronic Journal of Radiology. 2016;6(3):38–47. [Russian: Шабанова М.С. Сопоставление результатов измерения степени стенозирования просвета коронарных артерий при компьютерной томографии, внутрисосудистом ультразвуковом исследовании и коронарной ангиографии. Российский электронный журнал лучевой диагностики. 2016;6(3):38-47]. DOI: 10.21569/2222-7415-2016-6-3-38-47
8. Veselova T.N., Shabanova M.S., Mironov V.M., Merkulova I.N., Ternovoy S.K. Computed tomography in the evaluation of coronary atherosclerotic plaques: comparison with intravascular ultrasound. Kardiologiia. 2017;57(1):42–7. [Russian: Веселова Т.Н., Шабанова М.С., Миронов В.М., Меркулова И.Н., Терновой С.К. Компьютерная томоангиография коронарных артерий при сопоставлении с внутрисосудистым ультразвуковым исследованием. Кардиология. 2017;57(1):42-7]
9. Shariya M.A., Shabanova M.S., Veselova T.N., Merkulova I.N., Mironov V.M., Gaman S.A. et al. Comparison of computed tomography with intravascular ultrasound in evaluation of coronary plaques parameters. Medical Visualization. 2018;22(4):7–19. [Russian: Шария М.А., Шабанова М.С., Веселова Т.Н., Меркулова И.Н., Миронов В.М., Гаман С.А. и др. Сопоставление результатов компьютерной ангиографии и внутрисосудистого ультразвукового исследования в оценке параметров атеросклеротических бляшек. Медицинская визуализация. 2018;22(4):7-19]. DOI: 10.24835/1607-0763-2018-4-7-19
10. Abdulla J, Asferg C, Kofoed KF. Prognostic value of absence or presence of coronary artery disease determined by 64-slice computed tomography coronary angiography A systematic review and meta-analysis. The International Journal of Cardiovascular Imaging. 2011;27(3):413–20. DOI: 10.1007/s10554-010-9652-x
11. Tagieva N.R., Shakhnovich R.M., Mironov V.M., Ezhov M.V., Matchin Yu.G., Mitroshkin M.G. et al. Comparison of Atherosclerotic Lesions in Patients With Acute Myocardial Infarction and Stable Angina Pectoris Using Intravascular Ultrasound. Kardiologiia. 2015;55(7):5–13. [Russian: Тагиева Н.Р., Шахнович Р.М., Миронов В.М., Ежов М.В., Матчин Ю.Г., Митрошкин М.Г. и др. Сравнение атеросклеротических поражений коронарных артерий у больных острым инфарктом миокарда и стабильной стенокардией по данным внутрисосудистого ультразвукового исследования. Кардиология. 2015;55(7):5-13]
12. Yamaki T, Kawasaki M, Jang I-K, Raffel OC, Ishihara Y, Okubo M et al. Comparison between integrated backscatter intravascular ultrasound and 64-slice multi-detector row computed tomography for tissue characterization and volumetric assessment of coronary plaques. Cardiovascular Ultrasound. 2012;10(1):33. DOI: 10.1186/1476-7120-10-33
13. Obaid DR, Calvert PA, Brown A, Gopalan D, West NEJ, Rudd JHF et al. Coronary CT angiography features of ruptured and high-risk atherosclerotic plaques: Correlation with intra-vascular ultrasound. Journal of Cardiovascular Computed Tomography. 2017;11(6):455–61. DOI: 10.1016/j.jcct.2017.09.001
14. Marwan M, Taher MA, El Meniawy K, Awadallah H, Pflederer T, Schuhbäck A et al. In vivo CT detection of lipid-rich coronary artery atherosclerotic plaques using quantitative histogram analysis: A head to head comparison with IVUS. Atherosclerosis. 2011;215(1):110–5. DOI: 10.1016/j.atherosclerosis.2010.12.006
15. Pohle K, Achenbach S, MacNeill B, Ropers D, Ferencik M, Moselewski F et al. Characterization of non-calcified coronary atherosclerotic plaque by multi-detector row CT: Comparison to IVUS. Atherosclerosis. 2007;190(1):174–80. DOI: 10.1016/j.atherosclerosis.2006.01.013
16. Voros S, Rinehart S, Qian Z, Vazquez G, Anderson H, Murrieta L et al. Prospective Validation of Standardized, 3-Dimensional, Quantitative Coronary Computed Tomographic Plaque Measurements Using Radiofrequency Backscatter Intravascular Ultrasound as Reference Standard in Intermediate Coronary Arterial Lesions. JACC: Cardiovascular Interventions. 2011;4(2):198–208. DOI: 10.1016/j.jcin.2010.10.008
17. Kitagawa T, Yamamoto H, Horiguchi J, Ohhashi N, Tadehara F, Shokawa T et al. Characterization of Noncalcified Coronary Plaques and Identification of Culprit Lesions in Patients With Acute Coronary Syndrome by 64-Slice Computed Tomography. JACC: Cardiovascular Imaging. 2009;2(2):153–60. DOI: 10.1016/j.jcmg.2008.09.015
18. Hoffmann U, Moselewski F, Nieman K, Jang I-K, Ferencik M, Rahman AM et al. Noninvasive Assessment of Plaque Morphology and Composition in Culprit and Stable Lesions in Acute Coronary Syndrome and Stable Lesions in Stable Angina by Multidetector Computed Tomography. Journal of the American College of Cardiology. 2006;47(8):1655–62. DOI: 10.1016/j.jacc.2006.01.041
19. Motoyama S, Kondo T, Sarai M, Sugiura A, Harigaya H, Sato T et al. Multislice Computed Tomographic Characteristics of Coronary Lesions in Acute Coronary Syndromes. Journal of the American College of Cardiology. 2007;50(4):319–26. DOI: 10.1016/j.jacc.2007.03.044
20. Pflederer T, Marwan M, Schepis T, Ropers D, Seltmann M, Muschiol G et al. Characterization of culprit lesions in acute coronary syndromes using coronary dual-source CT angiography. Atherosclerosis. 2010;211(2):437–44. DOI: 10.1016/j.atherosclerosis.2010.02.001
21. Puchner SB, Liu T, Mayrhofer T, Truong QA, Lee H, Fleg JL et al. High-Risk Plaque Detected on Coronary CT Angiography Predicts Acute Coronary Syndromes Independent of Significant Stenosis in Acute Chest Pain: results from the ROMICAT-II trial. Journal of the American College of Cardiology. 2014;64(7):684–92. DOI: 10.1016/j.jacc.2014.05.039
22. Maurovich-Horvat P, Ferencik M, Voros S, Merkely B, Hoffmann U. Comprehensive plaque assessment by coronary CT angiography. Nature Reviews Cardiology. 2014;11(7):390–402. DOI: 10.1038/nrcardio.2014.60
23. Otsuka K, Fukuda S, Tanaka A, Nakanishi K, Taguchi H, Yoshikawa J et al. Napkin-Ring Sign on Coronary CT Angiography for the Prediction of Acute Coronary Syndrome. JACC: Cardiovascular Imaging. 2013;6(4):448–57. DOI: 10.1016/j.jcmg.2012.09.016
24. Ferencik M, Schlett CL, Ghoshhajra BB, Kriegel MF, Joshi SB, Maurovich-Horvat P et al. A Computed Tomography-Based Coronary Lesion Score to Predict Acute Coronary Syndrome Among Patients With Acute Chest Pain and Significant Coronary Stenosis on Coronary Computed Tomographic Angiogram. The American Journal of Cardiology. 2012;110(2):183–9. DOI: 10.1016/j.amjcard.2012.02.066
25. Veselova T.N., Merkulova I.N., Barysheva N.A., Ternovoy S.K., Shariya M.A., Ruda M.Ya. Comparison of characteristics of atherosclerotic plaques in patients with acute coronary syndrome and stable ischemic heart disease: data of multispiral computed tomography. Kardiologiia. 2013;53(12):14–20. [Russian: Веселова Т.Н., Меркулова И.Н., Ба-

рышева Н.А., Терновой С.К., Шария М.А., Руда М.Я. Сравнение особенностей атеросклеротических бляшек в коронарных артериях у больных острым коронарным синдромом и стабильной формой ишемической болезни сердца по данным мультиспиральной компьютерной томографии. Кардиология. 2013;53(12):14-20]
26. Kashiwagi M, Tanaka A, Shimada K, Kitabata H, Komukai K, Nishiguchi T et al. Distribution, frequency and clinical implications of napkin-ring sign assessed by multidetector computed tomography. Journal of Cardiology. 2013;61(6):399–403. DOI: 10.1016/j.jjcc.2013.01.004
27. Kröner ESJ, van Velzen JE, Boogers MJ, Siebelink H-MJ, Schalij MJ, Kroft LJ et al. Positive Remodeling on Coronary Computed Tomography as a Marker for Plaque Vulnerability on Virtual Histology Intravascular Ultrasound. The American Journal of Cardiology. 2011;107(12):1725–9. DOI: 10.1016/j.amjcard.2011.02.337
28. Benedek T, Jako B, Benedek I. Plaque Quantification by Coronary CT and Intravascular Ultrasound Identifies a Low CT Density Core as a Marker of Plaque Instability in Acute Coronary Syndromes. International Heart Journal. 2014;55(1):22–8. DOI: 10.1536/ihj.13-213
29. Ozaki Y, Okumura M, Ismail TF, Motoyama S, Naruse H, Hattori K et al. Coronary CT angiographic characteristics of culprit lesions in acute coronary syndromes not related to plaque rupture as defined by optical coherence tomography and angioscopy. European Heart Journal. 2011;32(22):2814–23. DOI: 10.1093/eurheartj/ehr189
30. Nakazato R, Otake H, Konishi A, Iwasaki M, Koo B-K, Fukuya H et al. Atherosclerotic plaque characterization by CT angiography for identification of high-risk coronary artery lesions: a comparison to optical coherence tomography. European Heart Journal - Cardiovascular Imaging. 2015;16(4):373–9. DOI: 10.1093/ehjci/jeu188
31. Bittner DO, Mayrhofer T, Puchner SB, Lu MT, Maurovich-Horvat P, Ghemigian K et al. Coronary Computed Tomography Angiography-Specific Definitions of High-Risk Plaque Features Improve Detection of Acute Coronary Syndrome. Circulation. Cardiovascular Imaging. 2018;11(8):e007657. DOI: 10.1161/CIRCIMAGING.118.007657
32. Kashiwagi M, Tanaka A, Kitabata H, Tsujioka H, Kataiwa H, Komukai K et al. Feasibility of noninvasive assessment of thin-cap fibroatheroma by multidetector computed tomography. JACC. Cardiovascular imaging. 2009;2(12):1412–9. DOI: 10.1016/j.jcmg.2009.09.012
33. Yuan M, Wu H, Li R, Yu M, Dai X, Zhang J. The value of quantified plaque analysis by dual-source coronary CT angiography to detect vulnerable plaques: a comparison study with intravascular ultrasound. Quantitative Imaging in Medicine and Surgery. 2020;10(3):668–77. DOI: 10.21037/qims.2020.01.13
34. Maehara A, Cristea E, Mintz GS, Lansky AJ, Dressler O, Biro S et al. Definitions and Methodology for the Grayscale and Radiofrequency Intravascular Ultrasound and Coronary Angiographic Analyses. JACC: Cardiovascular Imaging. 2012;5(3):S1–9. DOI: 10.1016/j.jcmg.2011.11.019
35. Roffi M, Patrono C, Collet J-P, Mueller C, Valgimigli M, Andreotti F et al. 2015 ESC Guidelines for the management of acute coronary syndromes in patients presenting without persistent ST-segment elevation: Task Force for the Management of Acute Coronary Syndromes in Patients Presenting without Persistent ST-Segment Elevation of the European Society of Cardiology (ESC). European Heart Journal. 2016;37(3):267–315. DOI: 10.1093/eurheartj/ehv320
36. van Velzen JE, Schuijf JD, de Graaf FR, Nucifora G, Pundziute G, Jukema JW et al. Plaque type and composition as evaluated non-invasively by MSCT angiography and invasively by VH IVUS in relation to the degree of stenosis. Heart. 2009;95(24):1990–6. DOI: 10.1136/hrt.2009.176933
37. Otsuka F, Yasuda S, Noguchi T, Ishibashi-Ueda H. Pathology of coronary atherosclerosis and thrombosis. Cardiovascular Diagnosis and Therapy. 2016;6(4):396–408. DOI: 10.21037/cdt.2016.06.01
38. Tanaka A, Shimada K, Sano T, Namba M, Sakamoto T, Nishida Y et al. Multiple Plaque Rupture and C-Reactive Protein in Acute Myocardial Infarction. Journal of the American College of Cardiology. 2005;45(10):1594–9. DOI: 10.1016/j.jacc.2005.01.053
39. Vergallo R, Ren X, Yonetsu T, Kato K, Uemura S, Yu B et al. Pancoronary plaque vulnerability in patients with acute coronary syndrome and ruptured culprit plaque: A 3-vessel optical coherence tomography study. American Heart Journal. 2014;167(1):59–67. DOI: 10.1016/j.ahj.2013.10.011
40. Mauriello A, Sangiorgi G, Fratoni S, Palmieri G, Bonanno E, Anemona L et al. Diffuse and Active Inflammation Occurs in Both Vulnerable and Stable Plaques of the Entire Coronary Tree: a histopathologic study of patients dying of acute myocardial infarction. Journal of the American College of Cardiology. 2005;45(10):1585–93. DOI: 10.1016/j.jacc.2005.01.054
41. Asakura M, Ueda Y, Yamaguchi O, Adachi T, Hirayama A, Hori M et al. Extensive development of vulnerable plaques as a pan-coronary process in patients with myocardial infarction: an angioscopic study. Journal of the American College of Cardiology. 2001;37(5):1284–8. DOI: 10.1016/S0735-1097(01)01135-4
42. Achenbach S, Marwan M. Intracoronary Thrombus. Journal of Cardiovascular Computed Tomography. 2009;3(5):344–5. DOI: 10.1016/j.jcct.2009.06.009
43. Maurovich-Horvat P, Schlett CL, Alkadhi H, Nakano M, Stolzmann P, Vorpahl M et al. Differentiation of Early from Advanced Coronary Atherosclerotic Lesions: Systematic Comparison of CT, Intravascular US, and Optical Frequency Domain Imaging with Histopathologic Examination in ex Vivo Human Hearts. Radiology. 2012;265(2):393–401. DOI: 10.1148/radiol.12111891
44. Cheruvu PK, Finn AV, Gardner C, Caplan J, Goldstein J, Stone GW et al. Frequency and Distribution of Thin-Cap Fibroatheroma and Ruptured Plaques in Human Coronary Arteries. Journal of the American College of Cardiology. 2007;50(10):940–9. DOI: 10.1016/j.jacc.2007.04.086
45. Tavora F, Cresswell N, Li L, Fowler D, Burke A. Frequency of acute plaque ruptures and thin cap atheromas at sites of maximal stenosis. Arquivos Brasileiros De Cardiologia. 2010;94(2):153–9. DOI: 10.1590/s0066-782x2010000200003
46. Pundziute G, Schuijf JD, Jukema JW, Decramer I, Sarno G, Vanhoenacker PK et al. Evaluation of plaque characteristics in acute coronary syndromes: non-invasive assessment with multi-slice computed tomography and invasive evaluation with intravascular ultrasound radiofrequency data analysis. European Heart Journal. 2008;29(19):2373–81. DOI: 10.1093/eurheartj/ehn356
47. Liu J, Wang Z, Wang W, Li Q, Ma Y, Liu C et al. Feasibility of diagnosing unstable plaque in patients with acute coronary syndrome using iMap-IVUS. Journal of Zhejiang University. Science. B. 2015;16(11):924–30. DOI: 10.1631/jzus.B1500206
48. Wieringa WG, Lexis CPH, Lipsic E, van der Werf HW, Burgerhof JGM, Hagens VE et al. In vivo coronary lesion differentiation with computed tomography angiography and intravascular ultrasound as compared to optical coherence tomography. Journal of Cardiovascular Computed Tomography. 2017;11(2):111–8. DOI: 10.1016/j.jcct.2017.01.004
49. Matsumoto H, Watanabe S, Kyo E, Tsuji T, Ando Y, Otaki Y et al. Standardized volumetric plaque quantification and characterization from coronary CT angiography: a head-to-head comparison with invasive intravascular ultrasound. European Radiology. 2019;29(11):6129–39. DOI: 10.1007/s00330-019-06219-3
50. Conte E, Mushtaq S, Pontone G, Li Piani L, Ravagnani P, Galli S et al. Plaque quantification by coronary computed tomography angiography using intravascular ultrasound as a reference standard: a comparison between standard and last generation computed tomography scanners. European Heart Journal - Cardiovascular Imaging. 2019;21(2):191–201. DOI: 10.1093/ehjci/jez089
51. Park H-B, Lee BK, Shin S, Heo R, Arsanjani R, Kitslaar PH et al. Clinical Feasibility of 3D Automated Coronary Atherosclerotic Plaque Quantification Algorithm on Coronary Computed Tomography Angiography: Comparison with Intravascular Ultrasound. European Radiology. 2015;25(10):3073–83. DOI: 10.1007/s00330-015-3698-z
52. Kigka VI, Sakellarios A, Kyriakidis S, Rigas G, Athanasiou L, Siogkas P et al. A three-dimensional quantification of calcified and non-calcified plaques in coronary arteries based on computed tomography coronary angiography images: Comparison with expert's anno-

ISSN 0022-9040. Kardiologiia. 2020;60(12). DOI: 10.18087/cardio.2020.12.n1304

tations and virtual histology intravascular ultrasound. Computers in Biology and Medicine. 2019;113:103409. DOI: 10.1016/j.compbiomed.2019.103409
53. Kolossváry M, Park J, Bang J-I, Zhang J, Lee JM, Paeng JC et al. Identification of invasive and radionuclide imaging markers of coronary plaque vulnerability using radiomic analysis of coronary computed tomography angiography. European Heart Journal - Cardiovascular Imaging. 2019;20(11):1250–8. DOI: 10.1093/ehjci/jez033
54. Masuda T, Nakaura T, Funama Y, Okimoto T, Sato T, Higaki T et al. Machine-learning integration of CT histogram analysis to evaluate the composition of atherosclerotic plaques: Validation with IB-IVUS. Journal of Cardiovascular Computed Tomography. 2019;13(2):163–9. DOI: 10.1016/j.jcct.2018.10.018
55. Heo R, Park H-B, Lee BK, Shin S, Arsanjani R, Min JK et al. Optimal boundary detection method and window settings for coronary atherosclerotic plaque volume analysis in coronary computed tomography angiography: comparison with intravascular ultrasound. European Radiology. 2016;26(9):3190–8. DOI: 10.1007/s00330-015-4121-5
56. Murata N, Hiro T, Takayama T, Migita S, Morikawa T, Tamaki T et al. High shear stress on the coronary arterial wall is related to computed tomography-derived high-risk plaque: a three-dimensional computed tomography and color-coded tissue-characterizing intravascular ultrasonography study. Heart and Vessels. 2019;34(9):1429–39. DOI: 10.1007/s00380-019-01389-y
57. Ito T, Terashima M, Kaneda H, Nasu K, Matsuo H, Ehara M et al. Comparison of In Vivo Assessment of Vulnerable Plaque by 64-Slice Multislice Computed Tomography Versus Optical Coherence Tomography. The American Journal of Cardiology. 2011;107(9):1270–7. DOI: 10.1016/j.amjcard.2010.12.036
58. Tanaka A, Shimada K, Yoshida K, Jissyo S, Tanaka H, Sakamoto M et al. Non-Invasive Assessment of Plaque Rupture by 64-Slice Multidetector Computed Tomography - Comparison With Intravascular Ultrasound. Circulation Journal. 2008;72(8):1276–81. DOI: 10.1253/circj.72.1276